J|A|C|S
ARTICLES
Published on Web 12/03/2002

Solvent Coordination in Gas-Phase $[Mn\cdot(H_2O)_n]^{2+}$ and $[Mn\cdot(ROH)_n]^{2+}$ Complexes: Theory and Experiment

Hazel Cox, Glen Akibo-Betts, Rossana R. Wright, Nicholas R. Walker, Sharon Curtis, Bridgette Duncombe, and Anthony J. Stace*

Contribution from the School of Chemistry, Physics and Environmental Science, University of Sussex, Falmer, Brighton BN1 9QJ, U.K.

Received October 15, 2001

Abstract: An experimental gas-phase study of the intensities and fragmentation patterns of $[Mn\cdot(H_2O)_n]^{2+}$ and $[Mn\cdot(ROH)_n]^{2+}$ complexes shows the combinations $[Mn\cdot(H_2O)_4]^{2+}$ and $[Mn\cdot(ROH)_4]^{2+}$ to be stable. Evidence in complexes involving the alcohols methanol, ethanol, 1-propanol, and 2-propanol favors preferential fragmentation to $[Mn\cdot(ROH)_4]^{2+}$, whereas the fragmentation data for water is less clear. Supporting density functional calculations show that both $[Mn\cdot(H_2O)_4]^{2+}$ and $[Mn\cdot(MeOH)_4]^{2+}$ adopt stable tetrahedral configurations, similar to those proposed for biochemical systems where solvent availability and coordination is restricted. Calculated incremental binding energies show a gradual decline on going from one to six solvent molecules, with a step occurring between four and five molecules. The addition of further solvent molecules to the stable $[Mn\cdot(MeOH)_4]^{2+}$ unit shows a preference for $[Mn\cdot(MeOH)_4(MeOH)_{1,2}]^{2+}$ structures, where the extra molecules occupy hydrogen-bonded sites in the form of a secondary solvation shell. Very similar behavior is seen on the part of water. As part of an analysis of the experimental data, the calculations have explored the influence different spins states of Mn^{2+} have on solvent geometry. It is concluded that the experimental observations are best reproduced when the central Mn^{2+} ion is in the high-spin ^6S ground state. The results are also considered in terms of the biochemical activity of Mn^{2+} where the ion is capable of isomorphous substitution with Zn^{2+}, which itself exhibits a preference for tetrahedral coordination.

Introduction

The closed-shell ions Na^+, Mg^{2+}, and Zn^{2+} have all been the subject of recent theoretical studies where the coordination of small numbers of either water or methanol molecules has been investigated.[1−10] In each case, these calculations have examined the influence hydrogen bonding has on the competition between primary and secondary solvent shell formation. For Mg^{2+} it would appear that the most stable primary shell consists of an octahedral arrangement of six solvent molecules.[4,5] In contrast, the majority of calculations on Zn^{2+} favor a tetrahedral configuration of four water molecules,[5,7,9,10] with additional molecules occupying hydrogen-bonded sites in a secondary shell. For Na^+, semi-emperical calculations on $Na^+(CH_3OH)_6$ complexes at elevated temperatures[11] show there to be no octahedral configuration, but that the most frequently observed structure consists of a 4 + 2 configuration where two molecules form acceptor hydrogen bonds in an outer solvation shell. Since Na^+, Mg^{2+}, and Zn^{2+} all have closed-shell electron configurations, they do not impose on the ligands any geometric constraints in the form of partially occupied orbitals that might, for example, yield a crystal field stabilization energy (CFSE) or lead to Jahn−Teller distortion of the complex.[12] Therefore, coordination is influenced primarily by (i) the degree of charge transfer between the ligands and the ion; (ii) ligand−ligand interactions; (iii) hydrogen-bond strengths. In an aqueous medium, Na^+, Zn^{2+}, and Mg^{2+} are all found to be coordinated to six water or six methanol molecules;[13,14] thus, Zn^{2+} would appear to respond to an extended solvent lattice by changing the geometric arrangement of the primary solvation shell. Such behavior has been confirmed in recent calculations on the cluster $[Zn(H_2O)_6](H_2O)_6{}^{2+}$.[10] This situation contrasts, for example, with the biochemical behavior of Zn^{2+} where the ion is predominantly coordinated to tetrahedral sites.[15] In some respects, the biochemical environment could be likened to the

* Corresponding author. E-mail: a.j.stace@sussex.ac.uk.

(1) Lisy, J. M. *Int. Rev. Phys. Chem.* **1997**, *16*, 267.
(2) Bauschlicher, C., Jr.; Sodupe, M.; Partridge, H. *J. Chem. Phys.* **1992**, *96*, 4453.
(3) Bock, C. W.; Kaufman, A.; Glusker, J. P. *Inorg. Chem.* **1994**, *33*, 419.
(4) Glendening, E. D.; Feller, D. *J. Phys. Chem.* **1996**, *100*, 4790.
(5) Pavlov, M.; Siegbahn, P. E. M.; Sandstrom, M. *J. Phys. Chem. A* **1998**, *102*, 219.
(6) Pye, C. C.; Rudolp, W. W. *J. Phys. Chem. A* **1998**, *102*, 9933.
(7) Bock, C. W.; Kaufman Katz, A.; Glusker, J. P. *J. Am. Chem.. Soc.* **1995**, *117*, 3754.
(8) Kaufman Katz, A.; Glusker, J. P.; Beebe, S. A.; Bock, C. W. *J. Am. Chem. Soc.* **1996**, *118*, 5752.
(9) Dudev, T.; Lim, C. *J. Am. Chem. Soc.* **2000**, *122*, 11146.
(10) Diaz, N.; Suarez, D.; Merz, K. M., Jr. *Chem. Phys. Lett.* **2000**, *326*, 288.
(11) Cabarcos, O. M.; Weinheimer, C. J.; Lisy, J. M. *J. Phys. Chem. A* **1999**, *103*, 8777.
(12) Cotton, F. A.; Wilkinson, G. *Advanced Inorganic Chemistry*; Wiley: London, 1988.
(13) Burgess, J. *Metal Ions in Solution*; Wiley: London, 1978. Ohtaki, H.; Radnai, T. *Chem. Rev.* **1993**, *93*, 1157.
(14) Inada, Y.; Hayashi, H.; Sugimoto, K.-I.; Funahashi, S. *J. Phys. Chem.* **1999**, *103*, 1401.
(15) Frausto da Silva, J. J. R.; Williams, R. J. P. *The Biological Chemistry of the Elements*; Clarendon Press: Oxford, 1997.

10.1021/ja012367p CCC: $25.00

finite-sized solvent system, where a limited number of hydrogen-bonded ligands allows subtle second-order interactions to influence geometry.

Apart from crystallographic data on the coordination of Zn^{2+}, there are no complementary gas-phase experimental data to confirm a preference for tetrahedral geometry in the presence of small numbers of ligands. Experiments by Lisy et al.[1,11] on the gas-phase solvation of Na^+ have detected the presence of hydrogen bonding in complexes containing fewer than six water or methanol molecules—the implication being that some molecules occupy an outer solvation shell which is populated before the metal ion is fully coordinated (in the context of bulk solvation). Likewise, recent experiments on $[Mg.(H_2O)_n]^{2+}$ complexes in the gas phase have been interpreted in terms of a contribution from higher energy structures,[16−18] where one or more molecules occupy outer hydrogen-bonded sites. Finally, theoretical data have also been presented recently on the structures of $[Be(H_2O)_n]^{2+}$ complexes, where the most stable configuration at $n = 6$ corresponds to a $4 + 2$ arrangement of ligands.[19]

In addition to Zn^{2+}, another notable "closed-shell" transition-metal ion with a common oxidation state of 2 is Mn^{2+} (d^5, high-spin ^6S ground state). The term "closed shell" being used in the context of the spin state having zero CFSE.[12] In biochemical systems, Mn^{2+} is capable of isomorphous substitution with Zn^{2+}, which would suggest that the two ions should exhibit very similar patterns of coordination.[15] This is certainly true in aqueous solution where they both have first hydration shells that contain six water molecules;[13,14] however, no experimental investigations have been undertaken on the coordination of Mn^{2+} in the presence of small numbers of solvent molecules. However, Bock et al.[20] have published the results of detailed calculations on the solvent structure surrounding Mn^{2+} when in the presence of small numbers of hydrogen-bonded molecules.

For Mn^{2+} to act as an effective substitute for Zn^{2+} in the biochemical environment,[15] the former would need to exhibit tetrahedral coordination. Presented here are the results of a gas-phase study of complexes of the form $[Mn^{\cdot}(H_2O)_n]^{2+}$ and $[Mn^{\cdot}(ROH)_n]^{2+}$, where ROH represents either methanol, ethanol, or propanol (both isomers). The experimental results are in the form of ion intensities and fragmentation patterns, and taken together these data provide strong evidence for a stable four-coordinate primary solvation shell. Supporting density functional calculations show the primary shells of the high-spin $[Mn^{\cdot}(H_2O)_4]^{2+}$ and $[Mn^{\cdot}(CH_3OH)_4]^{2+}$ complexes to have tetrahedral geometries, with additional solvent molecules occupying hydrogen-bonded sites in a secondary shell. The calculations also show that the geometry of the primary solvent shell changes in response to changes in the spin state of Mn^{2+}.

Experimental Section

A detailed description of the instrumentation used for generation, resolution, and detection of the cluster beam has been provided in previous publications.[18,21,22] Briefly, argon carrier gas at a pressure of between 30 and 40 psi was passed through a custom-built reservoir containing solvent in its liquid state, enabling solvent molecules to enter the argon flow. Since the alcohols studied are comparatively volatile, it was necessary to cool the reservoir in ice to maintain the required concentration of solvent over an extended period of time. The mixture of argon and solvent vapor was then subjected to supersonic expansion through a pulsed conical nozzle, followed by collimation 2-cm downstream by a 1-mm-diameter skimmer. Midway between the expansion chamber and the mass spectrometer, the cluster beam passed over the mouth of a high-temperature effusion cell (DCA Instruments, EC-40-63-21) equipped with a crucible of pyrolytic boron nitride, in which metal vapor was generated. To maximize the surface area of metal, the cell was positioned at a slight angle ($\cong$30°) with respect to the vertical. Metal vapor was allowed to diffuse into the flight tube to create a region where the vapor and the cluster beam could interact. Earlier experiments using the "pick-up" technique showed that the presence of clusters in the beam of the form Ar_nL_m was essential to the success of the technique (see below).[21]

Signal intensities measured on the apparatus over a series of experiments have suggested that the optimal partial pressure of metal vapor is between 10^{-1} and 10^{-2} Torr. Above this pressure, disruption of the cluster beam results in reduced signal intensity, and at lower pressures the metal/solvent clusters signal decreases. For manganese, the above partial pressure was estimated from the observation that the effusion cell operated most effectively when the temperature was held at 1100 °C, as measured with a standard C-type thermocouple. Formation of neutral metal/solvent clusters results from the collision of metal atoms with argon/solvent clusters, with the energy from the collision being dispersed by the ejection of argon atoms. This latter step is essential since collisions might otherwise form species with high internal energies, which would break up immediately. A shutter at the exit of the effusion cell was used to confirm the identity of clusters containing manganese, and where a survey was performed of the relative intensities of parent ions of a given series, the difference was taken between the signal intensity with the shutter open and closed. This approach removed any contribution from background signal that was not dependent on material originating from the effusion cell.

The neutral metal/solvent clusters were ionized by 100 eV electrons within the ion source of a high-resolution, double-focusing mass spectrometer (VG ZAB-E) and were then accelerated by a potential of +5 kV. After passing through a field-free region, ions were selected according to their mass/charge ratio in a magnetic sector. A second field-free region separated the magnetic sector from an electrostatic analyzer (ESA), and the presence of a gas cell in this region permitted the collisional activation of size-selected parent ions. For many of the complexes discussed here, fragmentation processes were examined in two ways: (i) metastable decay promoted through residual internal energy remaining in the complexes after electron impact ionization and recorded in the absence of any collision gas (background pressure $\sim 10^{-9}$ mbar); (ii) collision-induced dissociation (CID) promoted through the presence of $\sim 10^{-6}$ mbar of air as a collision gas. Fragments arising from both processes were identified by scanning the ESA in the form of a MIKE (mass-analyzed ion kinetic energy) scan.[23] These scans were performed on doubly charged ions with kinetic energies of 10 keV, which allowed for straightforward detection and verification of fragment ions resulting from Coulomb explosion. Final ion detection took place at a Daly detector, where phase-sensitive detection was facilitated by a Stanford Research Systems SR850 lock-in amplifier.

Computational Details. The reported calculations were performed using the Amsterdam Density Functional (ADF) package,[24] in associa-

(16) Rodrigeuz-Cruz, S. E.; Jockusch, R. A.; Williams, E. R. *J. Am. Chem. Soc.* **1998**, *120*, 5842.
(17) Rodrigeuz-Cruz, S. E.; Jockusch, R. A.; Williams, E. R. *J. Am. Chem. Soc.* **1999**, *121*, 1986.
(18) Barran, P. E.; Walker, N. R.; Stace, A. J. *J. Chem. Phys.* **2000**, *112*, 6173.
(19) Vitorge, P.; Masella, M. *Chem. Phys. Lett.* **2000**, *332*, 367.
(20) Bock, C. W.; Katz, A. K.; Markham, G. D.; Glusker, J. P. *J. Am. Chem. Soc.* **1999**, *121*, 7360.
(21) Walker, N. R.; Wright, R. R.; Stace, A. J. *J. Am. Chem. Soc.* **1999**, *121*, 4837.
(22) Walker, N.; Dobson, M. P.; Wright, R. R.; Barran, P. E.; Murrell, J. N.; Stace, A. J. *J. Am. Chem. Soc.* **2000**, *121*, 11138.
(23) Cooks, R. G.; Beynon, J. H.; Caprioli, R. M.; Lester, G. R. *Metastable Ions*; Elsevier: Amsterdam, 1973.
(24) ADF 2.3.0 Theoretical Chemistry, Vrije Universiteit, Amsterdam.

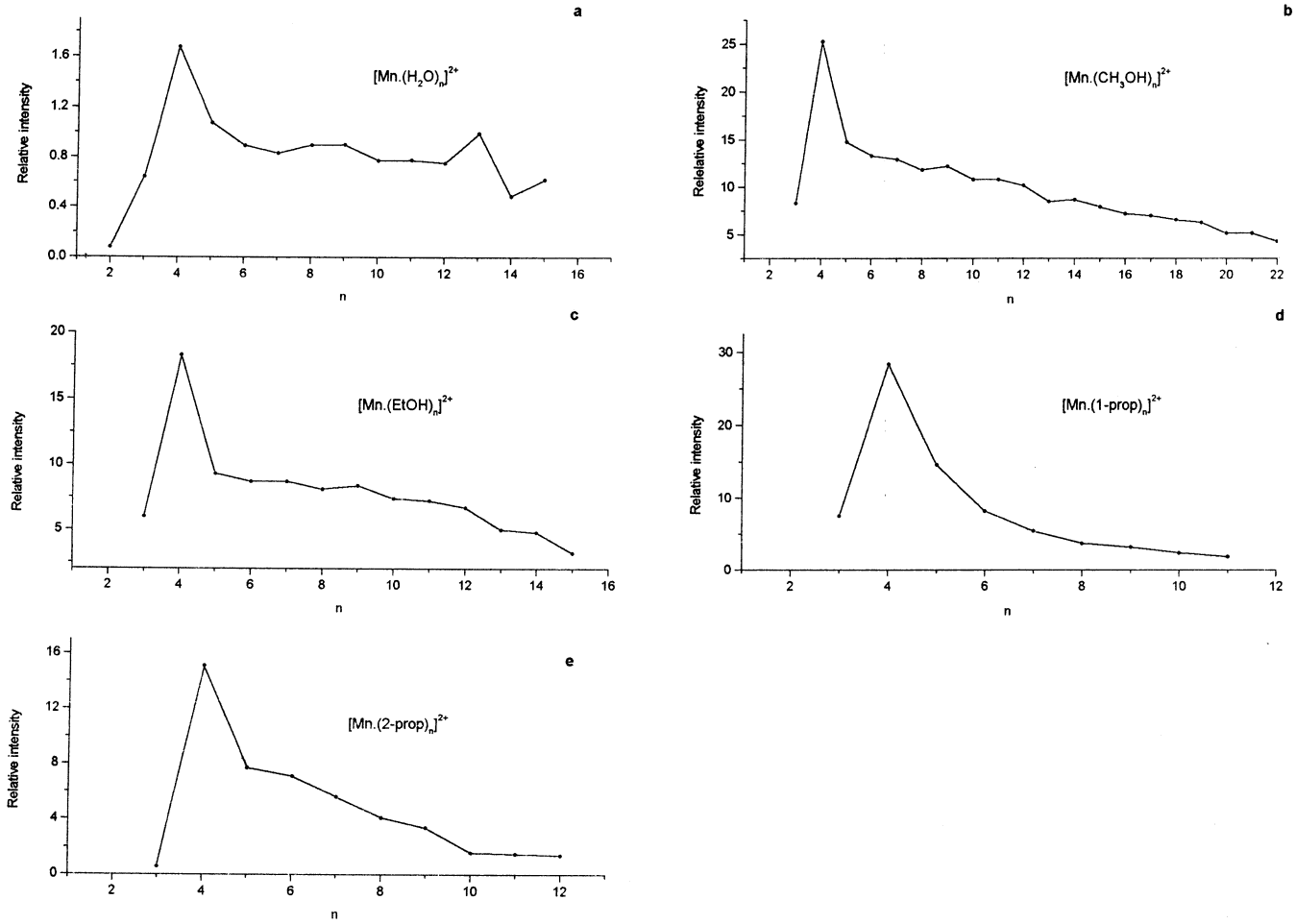

Figure 1. Relative intensity distributions recorded for the ions: (a) $[Mn\cdot(H_2O)_n]^{2+}$;(b) $[Mn\cdot(CH_3OH)_n]^{2+}$; (c) $[Mn\cdot(EtOH)_n]^{2+}$; (d) $[Mn\cdot(1\text{-prop})_n]^{2+}$; (e) $[Mn\cdot(2\text{-prop})_n]^{2+}$, as a function of *n*.

tion with the numerical integration procedure of te Velde and Baerends.[25] The energies of structures were calculated using the local density approximation (LDA) due to Vosko et al.,[26] with the nonlocal exchange terms of Becke,[27]and the nonlocal correlation correction of Perdew[28] being applied to the calculated LDA densities. A triple-ζ Slater-Type-Orbital (STO) basis set was used to describe the valence electrons of manganese. Hydrogen, oxygen, and carbon were described by double-ζ STOs augmented with polarization functions. The core atomic orbitals of manganese were set as [Ar] and treated using the frozen core approximation. Likewise, the 1s orbitals of carbon and oxygen were similarly treated as frozen cores.

Experimental Results. I. Intensity Distributions for Mn(II) Complexes. Figure 1 shows intensity distributions recorded for Mn(II) in association with the following solvent or ligand molecules (L): water, methanol, ethanol, 1-propanol, and 2-propanol. The weakest signals recorded were those of the $[Mn\cdot(H_2O)_n]^{2+}$ complexes; therefore, the corresponding data in Figure 1 represent an average of three separate measurements taken over a period of one week. The distributions shown in Figure 1 all contain a common feature, which is that, as a function of size, they peak sharply at $[Mn\cdot(L)_4]^{2+}$. An abrupt decline in intensity to $[Mn\cdot(L)_5]^{2+}$ is then followed in most cases by a comparatively gradual decrease in ion signal as a function of increasing cluster size. The interpretation of sharp fluctuations in signal intensity for ionic clusters has been discussed previously, and complexes such as $[Mn\cdot(CH_3OH)_4]^{2+}$ are believed to follow a pattern of behavior that is also thought to be responsible for the evolution of "magic numbers" in, for example, the mass spectra of rare gas clusters.[29] Following ionization and excitation by electron impact, comparatively unstable complexes fragment down to stable structures and the latter gain in intensity because of their reluctance to undergo further decay. On the basis of these ideas, it could be concluded from Figure 1 that for water and all four alcohols, $[Mn\cdot(L)_4]^{2+}$ is a particularly stable combination. The gradual decline in ion intensity beyond $[Mn\cdot(L)_5]^{2+}$ is consistent with other M^+ and M^{2+} systems where the solvent involved is capable of forming an extended network of hydrogen bonds.[30,31] Such behavior has previously been discussed in terms of the concentric shell model of ion solvation.[30,31]

II. Metastable Decay of Mn(II) Complexes. For each of the complexes, the process

$$[Mn\cdot(L)_n]^{2+} \rightarrow [Mn\cdot(L)_{n-1}]^{2+} + L \qquad (1)$$

was monitored via the appearance of an appropriate metastable fragment in the second field-free region of the mass spectrometer. Previous experiments on a range of cluster ions have shown the outcome of this reaction to be very sensitive to the presence of ions that are preferentially stable with respect to their immediate neighbors.[29,32] Figure 2 shows the results of measurements performed on ions for $n \leq 8$, where the intensity of each fragment ion has been normalized

(25) Te Velde, G.; Baerends, E. J. *J. Comput. Phys.* **1992**, *99*, 84.
(26) Vosko, S. H.; Wilk, L.; Nusair, N. *Can. J. Phys.* **1980**, *58*, 1200.
(27) Becke, A. D. *Phys Rev. A* **1988**, *38*, 3098.
(28) Perdew, J. P. *Phys Rev. B* **1986**, *33*, 8822.
(29) Lethbridge, P. G.; Stace, A. J. *J. Chem. Phys.* **1988**, *89*, 4062.
(30) Selegue, T. J.; Lisy, J. M. *J. Am. Chem. Soc.* **1994**, *116*, 4874.
(31) Woodward, C. A.; Dobson, M. P.; Stace, A. J. *J. Phys. Chem. A* **1997**, *101*, 2279.
(32) Stace, A. J.; Moore, C. *Chem. Phys. Lett.* **1983**, *96*, 80.

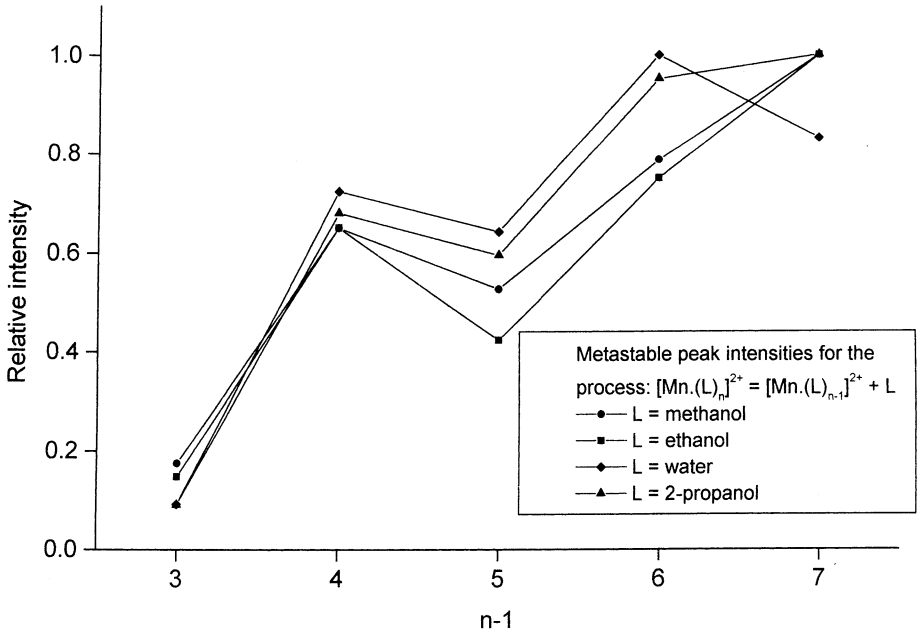

Figure 2. Relative intensities of metastable fragment ions from $[Mn\cdot(L)_n]^{2+}$ complexes undergoing reaction (1). The signals were recorded using the MIKE technique and have been normalized with respect to parent ion intensity. The data are plotted as a function of size, *n*.

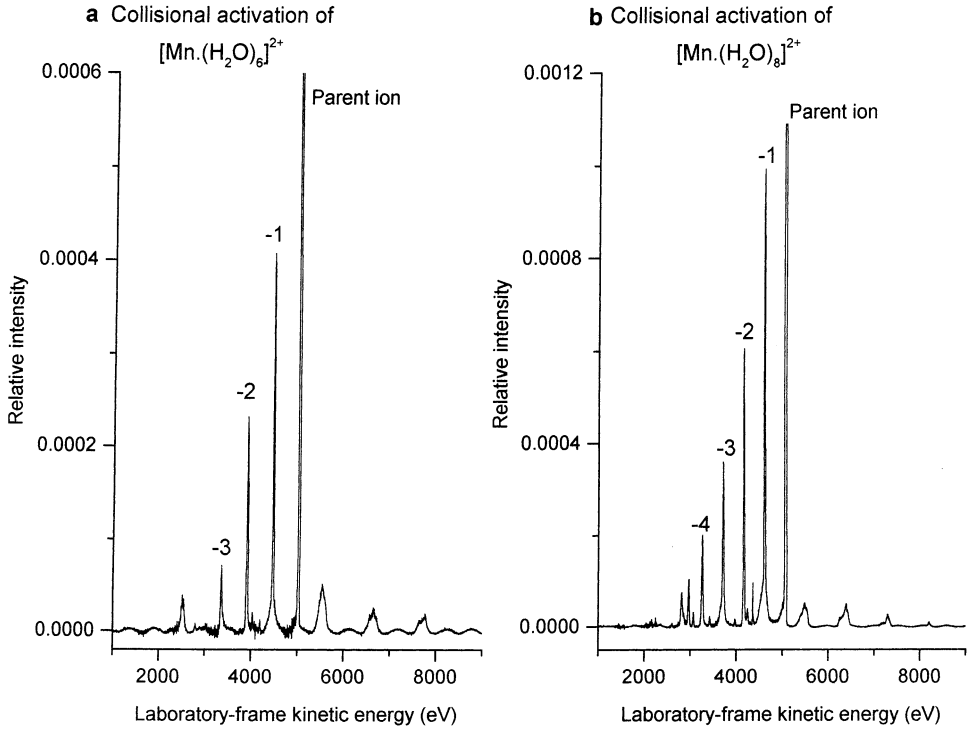

Figure 3. Relative intensities of fragment ions following the collisional activation of (a) $[Mn\cdot(H_2O)_6]^{2+}$ and (b) $[Mn\cdot(H_2O)_8]^{2+}$. The signals were recorded using the MIKE technique and are plotted as a function of laboratory-frame kinetic energy. The narrow peaks labeled −1, −2, etc. correspond to the loss of one and two neutral molecules, respectively, and the broader peaks correspond to charge-transfer processes.

with respect to the intensity of the parent (reliable intensity data could not be recorded for complexes involving 1-propanol). As expected, the overall trend in the data is that of a gradual increase in fragment intensity as a function of size; however, all of the examples exhibit a peak at $n - 1 = 4$ that could be indicative of preferential fragmentation to a stable metal−solvent structure of that composition.

III. MIKE Spectra of Mn(II) Complexes under CID Conditions. A small selection of fragmentation patterns recorded in the presence of a collision gas (air) are shown in figures 3−5 for size-selected $[Mn\cdot(H_2O)_n]^{2+}$ and $[Mn\cdot(ROH)_n]^{2+}$ complexes. As can be seen, all of the $[Mn\cdot(ROH)_n]^{2+}$ ions containing more than four molecules of any of the alcohols exhibit a very strong tendency to fragment down as far as $[Mn\cdot(ROH)_4]^{2+}$, but stop abruptly at that point. As noted by Blades et al.,[33] a sharp drop in fragment intensity, as seen, for example, in Figure 5b, could be equated with an increase in solvent-binding energy. Although $[Mn\cdot(ROH)_4]^{2+}$ ions do show some evidence of neutral ligand loss, which is to be expected since $[Mn\cdot(ROH)_3]^{2+}$ is also observed, the level of fragmentation is reduced, and the principal response from these ions to collisional activation is to undergo charge transfer. Stable,

(33) Blades, A. T.; Jayaweera, P.; Ikonomou, M. G.; Kebarle, P. *Int. J. Mass Spectrom. Ion Processes* **1990**, *102*, 251.

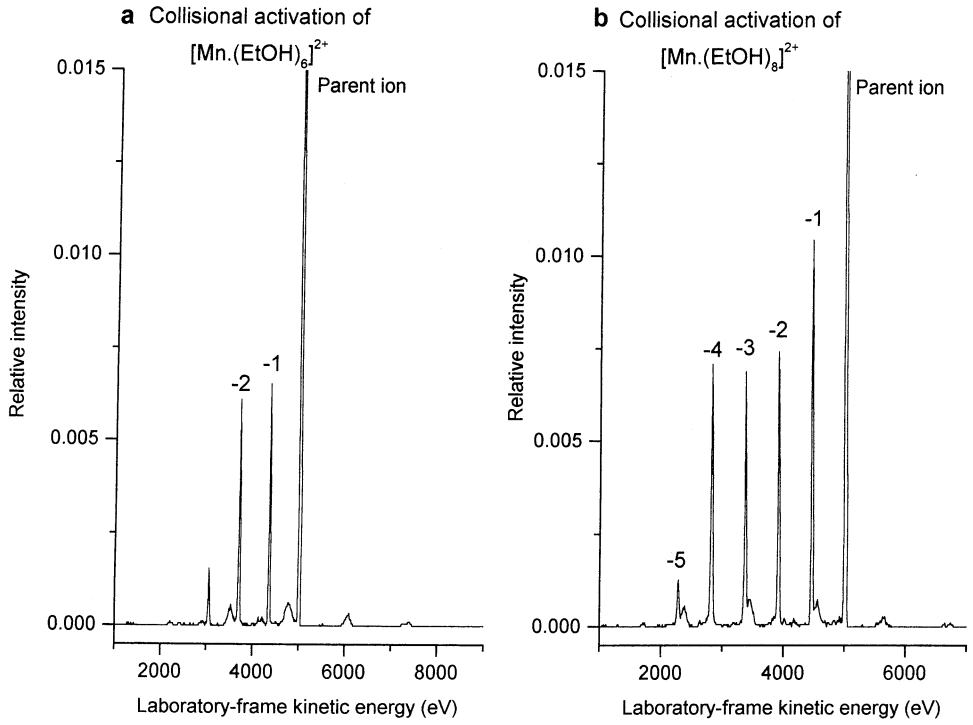

Figure 4. As for Figure 3, but for (a) $[Mn\cdot(EtOH)_6]^{2+}$ and (b) $[Mn\cdot(EtOH)_8]^{2+}$.

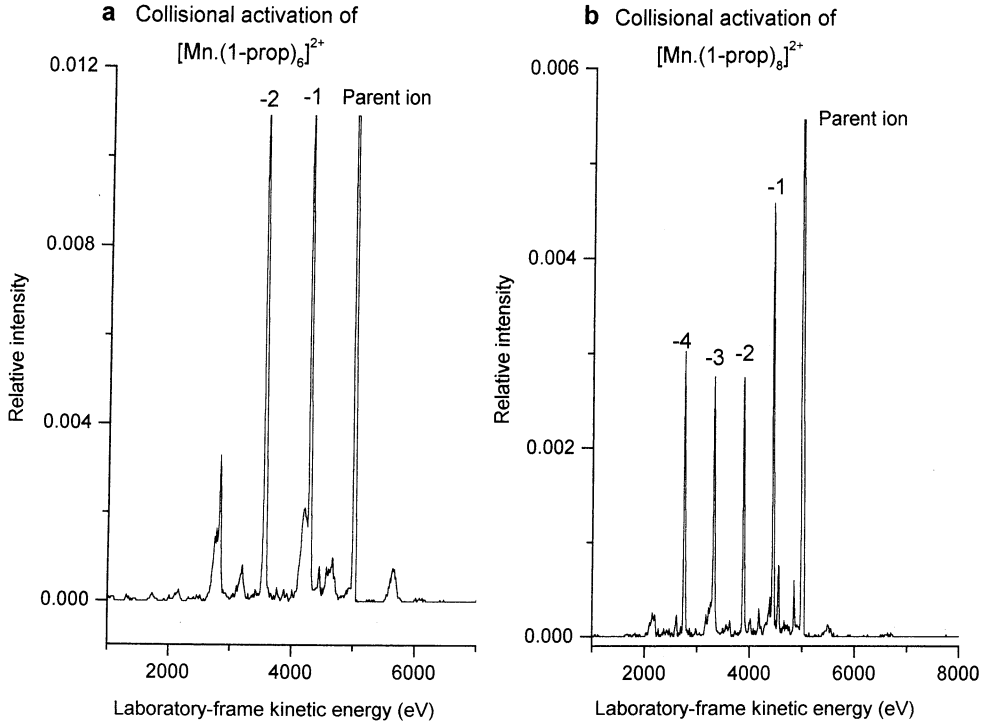

Figure 5. As for Figure 3, but for (a) $[Mn\cdot(1\text{-prop})_6]^{2+}$ and (b) $[Mn\cdot(1\text{-prop})_8]^{2+}$.

$[Mn\cdot(ROH)_3]^{2+}$ ions show no evidence of ligand loss as a result of collisional excitation but instead exhibit extensive charge transfer.[34] The fragmentation patterns seen for $[Mn\cdot(H_2O)_n]^{2+}$ complexes are slightly different from those of the alcohol-containing ions, in that the evidence for preferential fragmentation to $[Mn\cdot(H_2O)_4]^{2+}$ following collisional activation is less conclusive. Overall, these observations on fragmentation patterns provide further support for the conclusion reached following analysis of the ion intensity data, namely, that ions of the form $[Mn\cdot(ROH)_4]^{2+}$ (and possibly $[Mn\cdot(H_2O)_4]^{2+}$) would appear to be preferentially stable with respect to their immediate neighbors.

Computational Results. Geometry optimizations have been undertaken on a range of isomers of $[Mn\cdot(H_2O)_n]^{2+}$ and $[Mn\cdot(MeOH)_n]^{2+}$ clusters for $n \leq 6$. The stable structures identified from these calculations are used as the basis of a more general discussion covering all of the Mn^{2+}/solvent combinations that have been the subject of experimental study. The objective is to interpret the experimental data by investigating the energetics and possible geometries of the clusters involved. Given the high electron impact energy at which the neutral

(34) Walker, N. R. D. Philos. Thesis, University of Sussex, 1999.

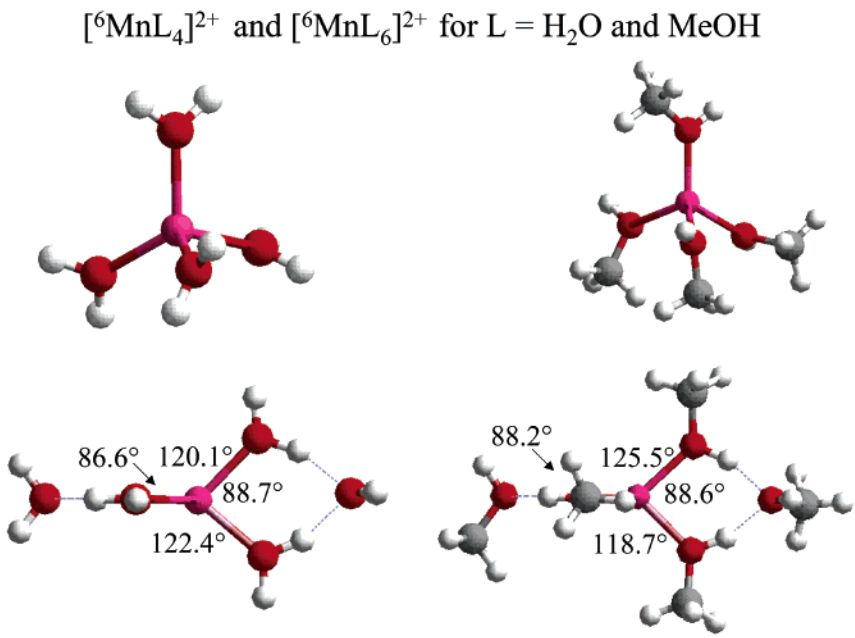

Figure 6. Stable structures calculated for $[Mn\cdot(H_2O)_{4,6}]^{2+}$ and $[Mn\cdot(CH_3OH)_{4,6}]^{2+}$ complexes with the Mn^{2+} ion in the high-spin ^6S state. In each of the two lower structures, one of the solvent molecules coordinated directly to the metal ion is obscured because of the angle of the projection.

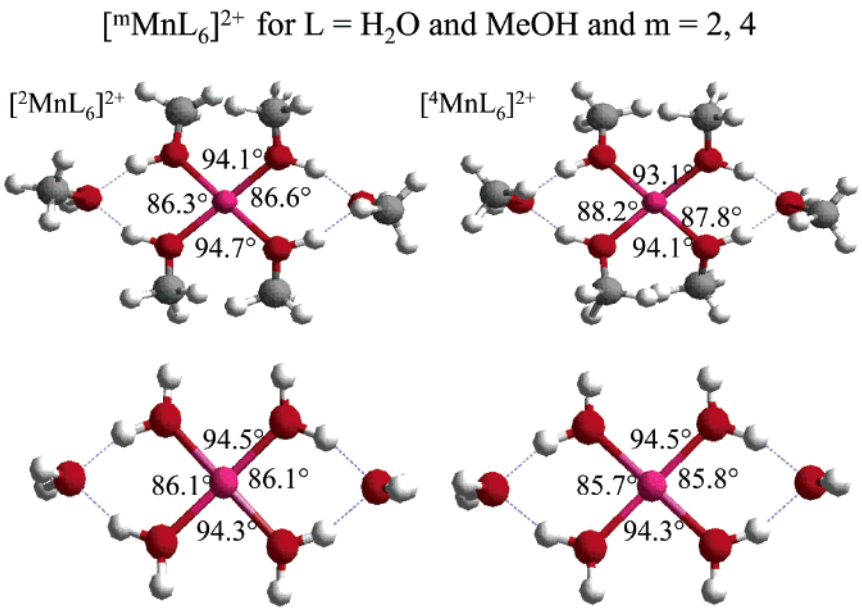

Figure 7. Stable structures calculated for $[Mn\cdot(H_2O)_6]^{2+}$ and $[Mn\cdot(CH_3OH)_6]^{2+}$ complexes with the Mn^{2+} ion in either the low-spin ^2I state or the intermediate ^4G state.

metal/solvent clusters are ionized (100 eV), it is quite probable that low- and intermediate-spin states of Mn^{2+} are accessed during an experiment. Therefore, it was considered necessary to explore the consequences of excited-state generation, and calculations have been performed on complexes containing the metal ion in the doublet (^2I, low-spin), the quartet (^4G, intermediate-spin), and the sextet state (^6S, high-spin ground state). A point of reference with regard to the examples present here is $[Mn\cdot(H_2O)_6]^{2+}$, which in the condensed phase is a high-spin complex.[12] The only notable condensed-phase low-spin complex is $[Mn\cdot(CN)_6]^{4-}$, where the ^2I state is stabilized by a ligand which occupies a much higher position than water in the spectrochemical series.[12] There is also evidence of low- and intermediate-spin complexes that are only stable at low temperatures.[35,36] Previous work in the condensed phase has also identified a series of stable Mn(II) complexes which contain alcohol molecules as ligands,[37] and these include some of those molecules studied here. Although no information appears to be available on ligand coordination, limited magnetic moment measurements on some of the complexes reveal that they contain five unpaired electrons.[38]

Figure 6 presents optimized structures calculated for $[Mn\cdot(L)_4]^{2+}$ and $[Mn\cdot(L)_6]^{2+}$ clusters (L = water or methanol) with the central metal ion in the ^6S spin state. Figure 7 shows optimized structures calculated for $[Mn\cdot(L)_6]^{2+}$ clusters with the metal ion in either the ^2I or ^4G spin state. In all cases, the final geometry is strongly dependent on the spin state; all doublet and quartet complexes are approximately square planar,

(35) Even, S.; Green, M. L. H.; Jewitt, B.; King, G. H.; Orchard, A. F. *J. Chem. Soc., Faraday Trans. 2* **1974**, *70*, 356.

(36) Robbins, J. L.; Edelstein, N. M.; Cooper, S. R.; Smart, J. C. *J. Am. Chem. Soc.* **1979**, *101*, 3853.

(37) Druce, J. G. F. *J. Chem. Soc.* **1937**, 1407.

(38) Gomer, R.; Tyson, G. N., Jr. *J. Am. Chem. Soc.* **1944**, *66*, 1331.

Table 1. Calculated Average Binding Energy, E_{av}, as Defined by Eq 1 for Each of the Complexes Listed in Association with Mn(II) in One of Three Spin States

complex	average binding energy/kJ mol^{-1}		
	doublet (^{2}I)	quartet (^{4}G)	sextet (^{6}S)
$[Mn\cdot(MeOH)_1]^{2+}$	711	625	412
$[Mn\cdot(MeOH)_2]^{2+}$	1023	901	731
$[Mn\cdot(MeOH)_3]^{2+}$	1243	1146	935
$[Mn\cdot(MeOH)_4]^{2+}$	1440	1340	1090
$[Mn\cdot(MeOH)_5]^{2+}$	1535	1426	1193
$\{[Mn\cdot(MeOH)_4]\ MeOH\}^{2+}$	1570	1466	1212
$[Mn\cdot(MeOH)_6]^{2+}$	1639	1511	1284
$\{[Mn\cdot(MeOH)_4](MeOH)_2\}^{2+}$	1702	1595	1332
$[Mn\cdot(H_2O)_1]^{2+}$	612	511	328
$[Mn\cdot(H_2O)_2]^{2+}$	876	774	608
$[Mn\cdot(H_2O)_3]^{2+}$	1102	1001	809
$[Mn\cdot(H_2O)_4]^{2+}$	1302	1200	973
$[Mn\cdot(H_2O)_5]^{2+}$	1412	1308	1086
$\{[Mn\cdot(H_2O)_4]\ H_2O\}^{2+}$	1441	1264	1092
$[Mn\cdot(H_2O)_6]^{2+}$	1519	1385	1184
$\{[Mn\cdot(H_2O)_4](H_2O)_2\}^{2+}$	1561	1465	1208

Table 2. Calculated Total Energy for Each of the Complexes Listed in Association with Mn(II) in One of Three Spin States

complex	total energy/kJ mol^{-1}		
	doublet (^{2}I)	quartet (^{4}G)	sextet (^{6}S)
$[Mn\cdot(MeOH)_1]^{2+}$	−1265	−1368	−1530
$[Mn\cdot(MeOH)_2]^{2+}$	−4441	−4507	−4711
$[Mn\cdot(MeOH)_3]^{2+}$	−7524	−7615	−7778
$[Mn\cdot(MeOH)_4]^{2+}$	−10583	−10672	−10797
$[Mn\cdot(MeOH)_5]^{2+}$	−13542	−13621	−13763
$\{[Mn\cdot(MeOH)_4]\ MeOH\}^{2+}$	−13576	−13661	−16782
$[Mn\cdot(MeOH)_6]^{2+}$	−16508	−16569	−16716
$\{[Mn\cdot(MeOH)_4](MeOH)_2\}^{2+}$	−16572	−16653	−16764
$[Mn\cdot(H_2O)_1]^{2+}$	349	261	70
$[Mn\cdot(H_2O)_2]^{2+}$	−1262	−1348	−1557
$[Mn\cdot(H_2O)_3]^{2+}$	−2835	−2923	−3105
$[Mn\cdot(H_2O)_4]^{2+}$	−4382	−4469	−4616
$[Mn\cdot(H_2O)_5]^{2+}$	−5840	−5923	−6076
$\{[Mn\cdot(H_2O)_4]\ H2O\}^{2+}$	−5868	−5880	−6083
$[Mn\cdot(H_2O)_6]^{2+}$	−7293	−7348	−7522
$\{[Mn\cdot(H_2O)_4](H_2O)_2\}^{2+}$	−7336	−7428	−7546

and all sextet complexes are approximately tetrahedral. This pattern of behavior can be understood in terms of the energy gained through crystal field stabilization (CFSE).[12] For a high-spin d^5 metal ion complex, there is no contribution from CFSE, and therefore, the ligands will adopt positions that minimize the degree of through-space repulsion. Hence, the sextet $[Mn\cdot(H_2O)_4]^{2+}$ and $[Mn\cdot(MeOH)_4]^{2+}$ complexes have tetrahedral geometries. In contrast, both the low- and intermediate-spin complexes gain from CFSE,[12] and this contribution is greater for a square-planar geometry than if the complexes were to adopt a tetrahedral configuration. Indeed, the CFSE prediction is that, in terms of binding energies, low-spin states should be the most stable for all $[Mn\cdot(L)_n]^{2+}$ complexes for $n \leq 6$. Table 1 shows the calculated average binding energy, E_{av}, for each of the $[Mn\cdot(L)_n]^{2+}$ (L = water or methanol) combinations examined here. These energies have been determined from the reaction equation:

$$Mn^{2+} + nL \rightarrow [Mn\cdot(L)_n]^{2+} \qquad (2)$$

As can be seen, the ordering of binding energies for $[Mn\cdot(L)_4]^{2+}$ complexes in the geometries determined by the various spin states follows the prediction given above. The high-spin complexes are always the least stable with respect to CFSE, and the ordering of the other two states follows the trend expected from CFSE. Indeed, the calculated binding energies for all of the $[Mn\cdot(L)_n]^{2+}$ complexes follow the trend predicted by CFSE.

However, this is not the complete picture, because account also needs to be taken of the energy required to create and maintain spin pairs in the excited ^{2}I and ^{4}G states of the Mn^{2+} ion.[39] When this contribution is taken into account in terms of a calculated total energy, which is given in Table 2, it can be seen that the $[Mn\cdot(L)_n]^{2+}$ sextet states are now energetically the most favorable and the doublet states the least favorable; an observation that matches existing data on condensed-phase Mn(II) complexes, which are predominantly high spin. The calculations suggest that the dimer complex $[Mn\cdot H_2O]^{2+}$ is unstable with respect to charge transfer. In these experiments, the minimum size of stable complex observed contained at least two solvent molecules; however, using an electrospray source, Shvartsburg and Siu have reported the detection of $[Mn\cdot H_2O]^{2+}$.[40]

Although it can be concluded from these calculations that high-spin $[Mn\cdot(L)_n]^{2+}$ complexes are going to be the most stable, it is not clear what the fate of excited states (if any) might be on the time scale of the experiment ($\sim 10^{-4}$ s). As with the optical spectroscopy of Mn(II), such decay processes would be spin-forbidden; however, they may be greatly assisted by both a high level of vibrational excitation and the fact that each centro-symmetric excited state is decaying to a noncentro-symmetric ground state.

For $n > 4$, there are two possible configurations: (a) the primary solvation shell can continue to fill until $n = 6$; or (b) as has been seen in small Be(II) and Zn(II) complexes,[5,7,9,10,19] additional molecules form double acceptor hydrogen bonds with the ligands in the primary solvation shell to create a second solvation shell. Referring to the binding energies given in Table 1, it can be seen that for all spin states the preferred arrangement is of the form $[Mn\cdot(L)_4\ (L)_{n-4}]^{2+}$ where for $n = 5$ and 6, molecules occupy a second solvation shell. The energy differences between $[Mn\cdot(L)_5]^{2+}$ and $[Mn\cdot(L)_4\ (L)]^{2+}$ are L = methanol 19 kJ mol^{-1} (^{6}S) and 35 kJ (^{2}I) mol^{-1}; and for L = water the corresponding values are 6 kJ mol^{-1} and 29 kJ mol^{-1}, respectively. Comparing $[Mn\cdot(L)_6]^{2+}$ and $[Mn\cdot(L)_4(L)_2]^{2+}$ complexes, the energy differences are L = methanol 48 kJ mol^{-1} and 63 kJ mol^{-1}, respectively; and L = water 24 kJ mol^{-1} and 42 kJ mol^{-1}, respectively. These energy differences are significantly larger than those calculated for the equivalent Zn^{2+} configurations, which only involved water.[5,7,9] However, the binding energy differences are smaller than those determined recently for hydrated Be^{2+}.[19]

To a first approximation, each of the 4-fold structures preserves its spin-dependent geometry following addition of the hydrogen-bonded molecules. However, as Figures 6 and 7 show in the $[Mn\cdot(H_2O)_4(H_2O)_2]^{2+}$ and $[Mn\cdot(MeOH)_4(MeOH)_2]^{2+}$ complexes, the structures do undergo some distortion to accommodate the extra ligands. The angle subtended by the two oxygen atoms that form the double hydrogen bond is reduced to ≈86° regardless of spin state. Several points of interest are apparent from Figures 6 and 7: first, both the square planar and tetrahedral $[Mn\cdot(L)_4]^{2+}$ structures are able to accommodate two additional molecules in very similar hydrogen-bonded configurations; second, only for square-planar $[Mn\cdot(H_2O)_4(H_2O)_2]^{2+}$ is it possible to add two further molecules to positions similar to those occupied by the fifth and sixth water molecules. Such a configuration would be very similar to the structure proposed for $[Cu.(H_2O)_8]^{2+}$ by Berc and co-workers,[41] where a total of four water molecules could be accommodated in a second ring of hydrogen-bonded molecules (see below); finally, following the formation of $[Mn\cdot(MeOH)_4(MeOH)_2]^{2+}$ as either a low- or intermediate-spin complex, the next most favorable coordination site is probably going to be an axial site on the metal ion.

Figure 8 shows a plot of incremental binding energies, E_{inc}, which are defined by the reaction process:

$$[Mn(L)_{n-1}]^{2+} + L \rightarrow [Mn(L)_n]^{2+} \qquad (3)$$

and have been derived from the data given in Table 1. Many of the values presented are similar in magnitude to those calculated for Zn^{2+}

(39) Huheey, J. E.; Keiter, E. A.; Keiter, R. L. *Inorganic Chemistry*; Harper Collins: New York, 1993.
(40) Shvartsburg, A. A.; Siu, K. W. M. *J. Am. Chem. Soc.* In print.

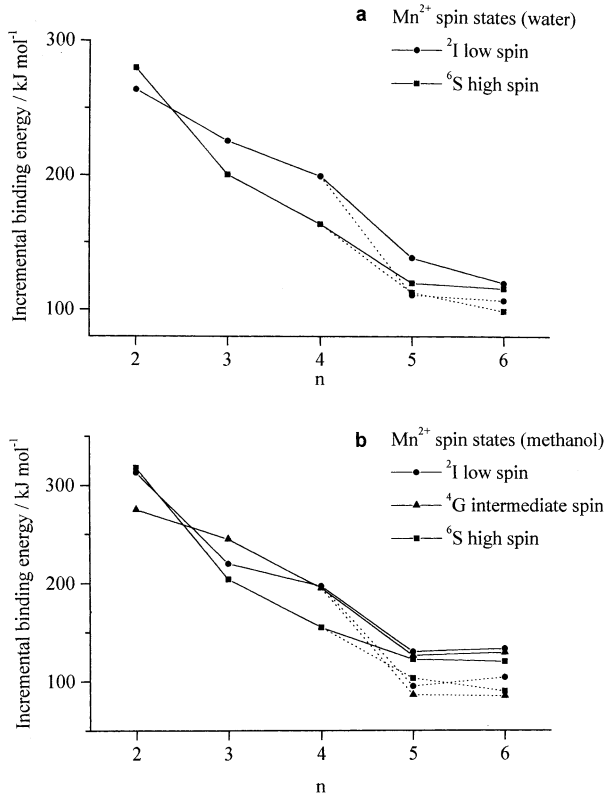

Figure 8. Calculated incremental binding energies for $[Mn\cdot(H_2O)_n]^{2+}$ and $[Mn\cdot(CH_3OH)_n]^{2+}$ complexes plotted as a function of *n*. Beyond $n = 4$, two separate routes are distinguishable for the addition of further molecules: complexes where the development of structure proceeds through the formation of hydrogen bonds (as seen in Figure 6) are denoted by a solid line, and complexes where the additional molecules are coordinated directly on to the metal ion are denoted by a dashed line. Data are presented for several of the Mn^{2+} spin states discussed in the text.

in association with water.[5,7,9] As might be anticipated from the data on total binding energies, beyond $n = 4$ there is a clear distinction between additional molecules going to hydrogen-bonded versus metal-ion sites, with the latter being the more weakly bound. Between pairs of complexes $[Mn\cdot(L)_5]^{2+}$ and $[Mn\cdot(L)_6]^{2+}$ (and in some cases between $[Mn\cdot(MeOH)_3]^{2+}$ and $[Mn\cdot(MeOH)_4]^{2+}$), there exist plateaus of stability, which are particularly pronounced for the doublet state. Similar behavior has been seen in calculations on $[Cu\cdot Ar_n]^{2+}$ and $[Ag\cdot Ar_n]^{2+}$ ions and was equated with stable primary-shell structures identified from measured ion intensities at $n = 4$ and $n = 6$.[42] Likewise in these experiments, if all large fragmenting complexes went via a route which took them through the most stable structures, then in addition to the $[Mn\cdot(L)_4]^{2+}$ ions already identified, comparatively intense ion signals might also have been anticipated for all $[Mn\cdot(L)_4\ (L)_2]^{2+}$ ions. However, in the $[Cu\cdot Ar_n]^{2+}$ and $[Ag\cdot Ar_n]^{2+}$ ions, all but the primary shell atoms were very weakly bound.[42] For the $[Mn\cdot(H_2O)_n]^{2+}$ and $[Mn\cdot(ROH)_n]^{2+}$ ions for $n > 4$, the small distinction in binding energy between those molecules that are either attached to the metal ion or hydrogen bonded at one or two sites is probably too subtle for its effect to be felt in these particular experiments. It is only when *n* is ≤ 4 (see below) that binding energy has a significant influence on events. Compounding the problem is the observation from experiments on $[Mg\cdot(H_2O)_n]^{2+}$ ions that a mixture of structures is to be expected.[16−18]

For all complexes in all spin states, the most significant change in binding energy to be experienced during downward fragmentation occurs between $[Mn\cdot(L)_5]^{2+}$ and $[Mn\cdot(L)_4]^{2+}$. If we consider the consequences of this result in terms of an *evaporative ensemble,* then the kinetic implications are quite clear.[43] To undergo the fragmentation step $[Mn\cdot(L)_5]^{2+} \rightarrow [Mn\cdot(L)_4]^{2+} + L$, the reactant ion would need to have at least 1 eV of internal energy. For the product ion to then undergo the next reaction step in this sequence requires, in some cases, an additional internal energy of at least twice that magnitude. Thus, $[Mn\cdot(L)_4]^{2+}$ would appear to be an obvious kinetic barrier to further fragmentation.

Further interesting details regarding the nature of the Mn^{2+}/methanol interaction emerge from a consideration of bond lengths and charge distributions. Figure 9 shows the variation in average Mn−O bond length for molecules in the first shell as a function of coordination number. Depending on how the molecules are coordinated, there are marked differences in behavior beyond $n = 4$. If the fifth and six molecules are hydrogen bonded in an outer shell, then the primary shell experiences a small decrease in Mn−O bond length. However, if the additional molecules occupy sites directly on the metal ion, then there is a significant increase in bond length. The spread in Mn(II)−O bond distances determined from experiments on hydrated cations is 2.18−2.2 Å,[13] which is very close to the values calculated here for the metal ion in 6-fold coordination. For the metal ion in 4-fold coordination, the bond distances can be expected to be significantly lower, and in this context experimental data given for crystal hydrates range from 2.0 to 2.18 Å.[44]

Complementing this observation are data on the charges that reside on the central metal ion and the coordinating oxygen atoms on the first-shell ligands. These data are plotted in Figure 10, where it can be seen that there are marked differences in behavior between complexes that develop a hydrogen-bonded solvent structure and those where additional ligands beyond $n = 4$ are directly bound to the metal ion. Of particular interest is the very significant decline in charge on the oxygen atoms in $[Mn\cdot(L)_6]^{2+}$ complexes. In contrast, the formation of $[Mn\cdot(L)_4\ (L)_2]^{2+}$ results in almost no change in charge either on the metal ion or the coordinating oxygen atoms. Results have been presented only for complexes containing the metal ion in the sextet state; however, very similar behavior is observed for the other two low-lying excited states of the metal ion.

If it is assumed that bonding between Mn^{2+} and small ligands, such as H_2O and CH_3OH is predominantly ionic, then the above observations fit to a single pattern. Octahedral coordination to the central metal ion reduces the magnitude of the charge anisotropy that exists between it and the oxygen atoms in the ligands. The resultant reduction in Coulomb attraction increases the metal−ligand bond length, which in turn leads to a reduction in binding energy. In contrast, tetrahedral coordination followed by hydrogen bonding maintains the charge anisotropy, which in turn keeps the bond lengths static and leads to a less rapid decline in binding energy. Therefore, a central $[Mn\cdot(L)_4]^{2+}$ core plays a significant role in determining the subsequent structure and behavior of larger clusters. The differences in behavior seen in Figures 9 and 10 between water and methanol can, for the most part, be attributed to the greater polarizability of methanol.

Discussion

The only other doubly charged ion to have been studied in similar experimental and theoretical detail in the gas phase is Cu(II).[41,45] This is fortuitous from the point of view of interpreting the results on Mn(II), since Cu(II) is known to form square-planar complexes in the condensed phase,[12] and recent calculations have also demonstrated a preference for such structures in the gas phase.[41] With reference to Table 3 where comparisons between data on Mn(II) and Cu(II) are made, it

(41) Berces, A.; Nukada, T.; Margl, P.; Ziegler, T. *J. Phys. Chem. A* **1999**, *103*, 9693.
(42) Walker, N. H. R.; Wright, R. R.; Barran, P. E.; Cox, H.; Stace, A. J. *J. Chem. Phys.* **2001**, *114*, 5562.
(43) Klots, C. E. *J. Chem. Phys.* **1985**, *83*, 5854.
(44) Burgess, J. *Ions in Solution*; Ellis Horwood: Chichester, 1988; p 40.
(45) Wright, R. R.; Walker, N. R.; Firth, S.; Stace, A. J. *J. Phys. Chem. A* **2001**, *105*, 54.

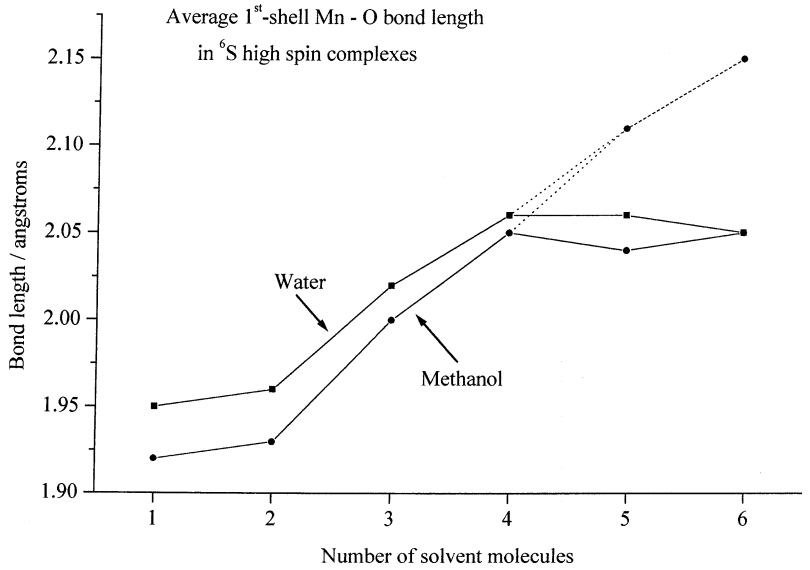

Figure 9. Calculated average Mn−O bond lengths for molecules in the first solvation shell of $[Mn\cdot(H_2O)_n]^{2+}$ and $[Mn\cdot(CH_3OH)_n]^{2+}$ complexes plotted as a function of *n*. Beyond $n = 4$, two separate routes are distinguishable for the addition of further molecules: complexes where the development of structure proceeds through the formation of hydrogen bonds (as seen in Figure 6) are denoted by a solid line, and complexes where the additional molecules are coordinated directly on to the metal ion are denoted by a dashed line. Data are presented for Mn^{2+} in the ^6S high-spin state.

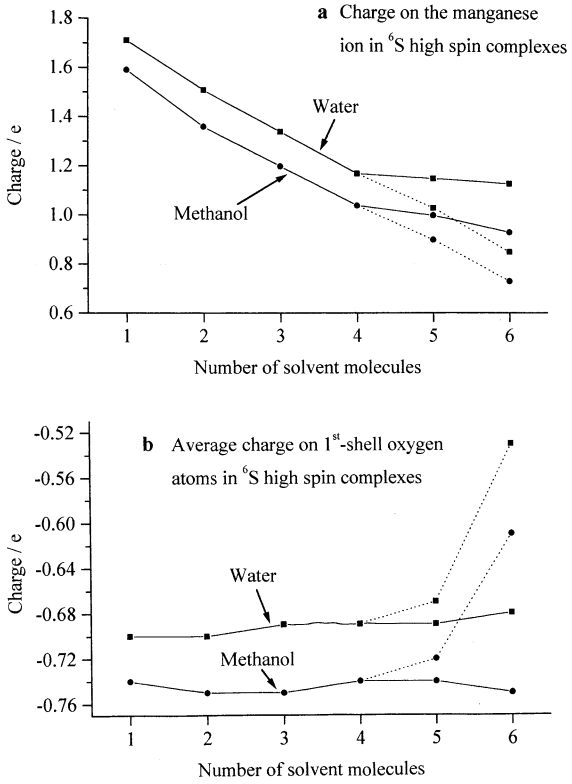

Figure 10. Average charge on (a) the manganese ion and (b) the oxygen atoms in $[Mn\cdot(H_2O)_n]^{2+}$ and $[Mn\cdot(CH_3OH)_n]^{2+}$ complexes plotted as a function of *n*. Beyond $n = 4$, two separate routes are distinguishable for the addition of further molecules: complexes where the development of structure proceeds through the formation of hydrogen bonds (as seen in Figure 6) are denoted by a solid line, and complexes where the additional molecules are coordinated directly on to the metal ion are denoted by a dashed line. Data are presented for Mn^{2+} in the ^6S high-spin state.

can be seen that there are significant differences between the two metal ions in terms of their coordination with water and alcohol molecules. As shown here, each $[Mn\cdot(L)_n]^{2+}$ complex exhibits an intensity profile that peaks sharply at $n = 4$; in contrast, the data for Cu(II) range from a maximum at $n = 8$ for water and methanol to 4-fold coordination for 1- and 2-propanol. The distinction between Cu(II) and Mn(II) becomes more dramatic when the difference in ionic radius is taken into consideration (see Table 3). On the basis of size, the larger radius of Mn(II) might have been expected to accommodate more ligands, but the trend in Table 3 is quite the reverse.

Table 3. Comparison of the Gas-Phase Solvation of Mn(II) and Cu(II) in Association with Alcohol Ligands.[45] Also Included Are Data on Ionic Radii and Hydration Enthalpies[13]

	intensity maximum	
ligand	manganese	copper
water	4	8
methanol	4	8
ethanol	4	6
1-propanol	4	4
2-propanol	4	4
ionic radius[a]	83/pm	57/pm
hydration enthalpy[a]	−1845/kJ mol^{-1}	−2099/kJ mol^{-1}

[a] The corresponding values for Zn^{2+} are 73 pm and −2044 kJ mol^{-1}.

Recent calculations on $[Cu\cdot(H_2O)_n]^{2+}$ ions have shown that the gas-phase structures adopted by these complexes develop in a manner which is different from that considered appropriate for the metal ion in solution.[12] Density functional calculations by Berce and co-workers[41] show the primary solvation shell to consist of four water molecules occupying equatorial sites in a square-planar configuration (an observation that is consistent with existing condensed-phase data on d^9 $[Cu.L_4]^{2+}$ complexes). However, additional water molecules do not occupy the two remaining axial sites, but instead prefer to extend the planar arrangement with up to four molecules, by forming double acceptor hydrogen bonds with the primary shell. For $n = 6$, these structures are very similar to those shown in Figure 7 for the low-spin $[Mn\cdot(H_2O)_6]^{2+}$ and $[Mn\cdot(MeOH)_6]^{2+}$ complexes; however, in contrast to $[Mn\cdot(H_2O)_6]^{2+}$, the equivalent structure formed between Cu(II) and water develops to form a very stable complex which can accommodate up to eight molecules. Experimental confirmation on the part of Cu(II) comes in the form of intensity measurements which suggest that both [Cu·

$(H_2O)_8]^{2+}$ and $[Cu\cdot(NH_3)_8]^{2+}$ are more stable than their immediate neighbors.[46,47] Such distributions are again a consequence of the kinetic aspects to the measurement procedure in these experiments. The axial sites on the metal ion can clearly accommodate water molecules; however, partly because of Jahn−Teller distortion, molecules occupying those sites are less strongly bound than those that form hydrogen bonds in the secondary solvation shell.[41]

To extend the structures identified by Berce et al.[41] for the purposes of accounting for the intensity maximum seen for $[Cu\cdot(CH_3OH)_8]^{2+}$ would require each donor molecule to form just a single hydrogen bond with an inner-shell acceptor molecule. Other gas-phase experiments on both singly and doubly charged methanol/metal ion complexes have demonstrated that methanol readily forms these extended hydrogen-bonded networks, which in some cases contain twenty or more molecules.[1,11,30,31] Therefore, the square-planar structures identified here for low-spin Mn(II) complexes would suggest similar extended networks might have been expected on the part of $[Mn\cdot(MeOH)_n]^{2+}$ complexes if excited states were contributing to the experimental observations. The ion intensity data presented for $[Cu\cdot(EtOH)_n]^{2+}$ is also consistent with a square-planar arrangement as shown, for example, in Figure 7; but again the equivalent $[Mn\cdot(EtOH)_6]^{2+}$ is not seen as being particularly stable in the experimental data. Finally, it is quite possible that steric factors and a reduction in hydrogen-bond strength are responsible for the data on both $[Cu\cdot(1\text{-}PrOH)_n]^{2+}$ and $[Cu\cdot(2\text{-}PrOH)_n]^{2+}$ showing maxima at $n = 4$.

Overall, the differences between Cu(II) and Mn(II) would suggest that complexes involving the latter are not square-planar and are not, therefore, in either the ^2I or ^4G spin states. As we have already discussed, one possible reason for the difference in behavior between Cu(II) and Mn(II) is that complexes containing Mn(II) in the ^6S ground-state configuration have no crystal field stabilization energy. Therefore, ligands do not derive any preferential stability by adopting a particular stereochemistry and, as a consequence, are less strongly bound to Mn(II) than Cu(II). Their respective hydration enthalpies reflect this difference, as does the fact that the calculated incremental binding energies for $[Cu\cdot(H_2O)_{4,5}]^{2+} + H_2O$ are slightly larger than those calculated for $[Mn\cdot(H_2O)_{4,5}]^{2+} + H_2O$ and $[Mn\cdot(CH_3OH)_{4,5}]^{2+} + CH_3OH$. In contrast, the calculated binding energies for low-spin square-planar Mn(II) complexes are comparable to those of Cu(II). The results shown here would suggest that the absence of CFSE influences behavior in secondary solvation shells, as demonstrated by the inability of Mn(II) to form any type of extended hydrogen-bond network. However, it is also recognized that there is a significant difference in ionic radius between Mn(II) and Cu(II). The smaller value for the latter ion will lead to an increased contribution to binding from ion−dipole and ion−induced dipole interactions, both of which will be important for the relatively large polarizable alcohol molecules studied here.

At a qualitative level, the complexes would appear to conform well to the hard−soft−acid−base model of metal ion−ligand interactions.[13,48,49] These characteristics on the part of Mn(II) are very similar to those identified for $[Zn\cdot(H_2O)_n]^{2+}$ complexes in recent calculations.[7,9] There it was concluded that Zn(II) derives much of its biological activity from creating tightly bound tetrahedral sites which are ideally suited to stabilizing protein configurations. The fact that Mn(II) and Zn(II) can undergo isomorphous substitution underpins many of the conclusions discussed here.[15]

Conclusion

Three separate aspects of the experimental behavior of $[Mn\cdot(ROH)_n]^{2+}$ complexes have been examined: ion intensity, unimolecular (metastable) decay, and fragmentation following collisional activation. On the basis of these data, it has been proposed that complexes of the form $[Mn\cdot(ROH)_4]^{2+}$ are more stable than their immediate neighbors. Supporting density functional calculations show the primary solvation shells for isolated Mn^{2+} ions in the presence of ROH molecules to consist of four molecules in a tetrahedral arrangement. The calculations also show that additional molecules occupy hydrogen-bonded sites in a secondary shell leading to structures of the form $[Mn\cdot(ROH)_4\ (ROH)_{1,2}]^{2+}$.

Acknowledgment. The authors would like to thank EPSRC for financial assistance with the experimental program, for the award of studentships to GA-B, B.D., and S.C., and for the award of an Advanced Research Fellowship to H.C. All calculations were performed on an ONYX 2 belonging to the Sussex High Performance Computing Initiative.

JA012367P

(46) Stace, A. J.; Walker, N. R.; Firth, S. *J. Am. Chem. Soc.* **1997**, *119*, 10239.
(47) Walker, N. R.; Firth, S.; Stace, A. J. *Chem. Phys. Lett.* **1998**, *292*, 125.
(48) Ahrland, S.; Chatt, J.; Davies, N. R. *Quart. Rev.* **1958**, *12*, 265.
(49) *Hard and Soft Acids and Bases*; Pearson, R. G., Ed.; Dowden, Hutchinson and Ross: Stroudsburg, PA, 1973.